Biochimica et Biophysica Acta, 555 (1979) 316—336

BBA 78439

EXCHANGE AND INTERACTIONS BETWEEN LIPID LAYERS AT THE SURFACE OF A LIPOSOME SOLUTION

HANSGEORG SCHINDLER

Biozentrum, Department of Biophysical Chemistry, Klingelbergstrasse 70, CH-4056 Basel (Switzerland)

(Received December 27th, 1978)

Key words: Lipid exchange; Liposome-monolayer interaction; Lipid selforganization; Adhesion; Fusion; Surface activity

Summary

Lipid organization and lipid transport processes occurring at the air-water interface of a liposome (lipid vesicle) solution are studied by conventional surface pressure-area measurements and interpreted by an adequate theory. At the interface of a dioleoyl phosphatidylcholine vesicle solution, used for demonstration, a well defined two layer structure selfassembles: vesicles disintegrate at the interface forming a surface-adsorbed lipid monolayer, which prevents further disintegration beyond about 1 dyne/cm surface pressure. A layer of vesicles now assembles in close association with the monolayer. This layer is in vesicle diffusion exchange with the solution and in lipid exchange with the monolayer. The lipid exchange occurs exclusively between the monolayer and the outer lipid layer of the vesicles; it is absent between outer and inner vesicle layers. Equilibration of the lipid density in the monolayer with that in the vesicle outer layer provides a coherent and quantitative explanation of the observed hysteresis effects and equilibrium states. The correspondence between monolayer and vesicle outer layer is traced down to equilibrium constants and rate constants and their dependences on surface pressure, vesicle size and concentration.

Other alternate realizations of surface structure and exchange, including induced lipid flip-flop within vesicles or vesicle monolayer adhesion or fusion are potential applications of the proposed analysis.

Introduction

Liposomes or lipid vesicles have attracted much interest in recent years. Their applications range from membrane reconstitution studies [1] to their use

Abbreviation: DOPC, dioleoyl phosphatidylcholine.

as a tool for exploring important questions in cell biology and in experimental therapeutics, where the liposome serves as a carrier vehicle to introduce a variety of biologically active materials into cells or into the cell wall, either by interaction or fusion with the cell wall or by the uptake of intact vesicles by the cells (for a comprehensive collection of recent studies see Ref. 2).

The incorporation of functional membrane proteins into lipid vesicles has been quite successful [1]. Reconstitution of planar lipid-protein bilayers, which allow a detailed electrical characterization of the membrane, has comparatively, met with less success. However, recent developments indicate a profitable use of reconstituted vesicles in forming planar bilayers, either by fusion of vesicles to a preformed lipid bilayer [3] or by the association of two vesicle-spread lipid-protein monolayers [4].

Interactions and exchange between spatially independent structures certainly play the key role in these applications of liposomes. Modalities and models have been proposed for some of the various possible processes, such as for membrane fusion events [5—7] or lipid exchange [8]. Yet, more experimental effort is needed to unravel the actual molecular mechanisms of intermembrane processes. The main intention of this study is to show that the interfacial phase of a vesicle solution, a layer of vesicles in interaction with a lipid monolayer, may serve as a model system to study exchange and interactions between lipid layers. There are two virtues to this: first, this model system selfassembles at the surface of a vesicle solution. Second, the well-developed precise techniques to study surface films may be applied to characterize the vesicle-monolayer interactions. The pioneering demonstration of lipid monolayer formation from vesicles is due to Verger and coworkers [9,10]. Monolayers were formed from a vesicle solution spread out into a thin layer around a glass rod, one end of which was in contact with the surface of an aqueous phase. For the present investigation of the mechanism of vesicle spreading, another experimental approach seemed more advantageous: the selfassembly of a lipid phase at the interface of a homogeneous vesicle solution. The equilibrium and kinetic properties of the resulting interfacial lipid phase reveal detailed information about organization and rearrangements of lipids and vesicles within this interfacial phase.

Materials and Methods

Dioleoyl phosphatidylcholine (DOPC) was synthesized [11], analyzed for purity [12,13] and quantitated [14] as described. For the synthesis of ^{3}H-labelled DOPC, [^{3}H]oleic acid (purchased from The Radiochemical Centre Ltd., nominally labelled in the 9,10-positions and with a specific activity of 2.2 Ci/mmol) was added to unlabelled oleic acid (obtained from Fluka, puriss.) in the ratio 1 : 5000. Reagent grade sodium chloride was purchased from Merck.

Single bilayer vesicles were prepared by the injection method [15,16]. The vesicle size was determined by coherent light scattering [17]. It was reproducibly uniform when lipid concentrations of less than 25 mg/ml ethanol were used. For higher concentrations increasing size non-uniformity occurred. The

vesicle radius increased linearly from 23 ± 2 nm at 4 mg lipid/ml ethanol to 35 ± 2 at 20 mg/ml. Vesicles of these two sizes are exclusively used in the experiments presented. The corresponding diffusion coefficients are $9.5 \cdot 10^{-8}$ and $6.3 \cdot 10^{-8}$ cm^2/s. The vesicles were routinely controlled every few days by coherent light scattering; they usually were stable for at least two weeks.

All experiments were performed using a conventional Langmuir balance [18] of 60×16 cm^2 surface area, in which a small Teflon chamber (14×1 cm^2) for the vesicle solutions was inserted. Convection flow between vesicle solution and the adjacent aqueous solutions was minimized by small exchange areas (0.5% of the total common area). Surface pressures were measured with an accuracy of about 0.1 dyne/cm. The presented results are obtained with the following configurations:

Constant surface pressure. The vesicle chamber was placed between balance and surface barrier; the mutual distances were always larger than or equal to 1 cm. Upon filling the chamber with vesicle solution its surface was connected with the adjacent surfaces by use of a thin glass loop. Adjustment of the surface area at constant surface pressure condition was by hand.

Zero surface pressure. Surface adsorption at surface pressures close to zero was measured by introducing every few minutes an additional surface barrier half-way between vesicle chamber and balance. The barrier was moved towards the balance until a well measurable surface pressure developed, which allowed the lipid content at the surface to be estimated by means of the pressure-lipid area relation. Thereupon the compressed film was withdrawn, while equal amounts of aqueous solution were added, the barrier removed and again placed half-way between vesicle chamber and balance for the next estimate of the lipid adsorption.

Constant surface area. During measurements of the surface pressure at constant surface area another vesicle chamber was used: to one side it was closed, its second wall did not reach the water level and was placed underneath one edge of the balance.

Surface pressure-area curves. A vesicle chamber (its upper rim just below the surface) was placed at some distance from the balance but close to the surface barrier. The latter was moved over the vesicle chamber towards the balance. Surface pressure vs. area curves were then repeatedly recorded at certain rates of area change (typical value 10% of the initial area/min) until the traces stayed invariable.

Results

This study of vesicle-monolayer interactions is confined to dioleoyl phosphatidylcholine (DOPC) vesicles in 0.1 M NaCl aqueous solution at room temperature. The two main experimental parameters are vesicle concentration and vesicle size. The complete set of data from the different modes of operating the surface balance will be presented for one vesicle size (35 nm radius) at one concentration (0.37 mg/ml). Representative data at other concentrations are added. The vesicle size dependence of the results is investigated in a separate chapter.

Constant surface area

After the vesicle chamber is filled with a solution of certain vesicle concentration (cf. Materials and Methods for details) the surface pressure p at constant surface area is observed to rise in time. The time course of p strongly depends on the vesicle concentration, as shown in Fig. 1, and is characterized by a delayed sigmoidal fast pressure rise followed by a steady slow rise. These data suggest a vesicle concentration-independent steady-state pressure. However, the details of the slow rise, especially the final value of the surface pressure at low vesicle concentrations, varied for independent experiments (dotted part of the curves), which is probably due to small leakages across the barriers. The complex time course of the pressure rise suggests that the surface pressure rise depends on the surface pressure itself. Thus, experiments at constant surface pressure instead of constant surface area are the natural choice to analyze the lipid organization at the surface of a vesicle solution. However, the reproducible sigmoidic onset of the surface pressure at the different concentrations in Fig. 1 is used below for an independent test of the conclusions drawn from experiments at constant surface pressure.

Surface pressure-area relation

A lipid monolayer is commonly characterized by its relation between surface pressure (p) and area/lipid (A). The surface layer of a vesicle solution, however, cannot be described by a unique p-A relation because of hysteresis effects. However, a unique p-A relation is found if the surface layer is carefully moved towards a vesicle-free part of the trough (cf. Materials and Methods for details). The p-A relation, repeatedly recorded, approached within about 30 min the relation shown in Fig. 2a, during which all hysteresis effects vanished. Virtually identical curves were recorded under various conditions of vesicle size or concentration or surface pressure before displacement. Fig. 2b illustrates the change of the p-A relation as a function of time (after shifting the surface layer) for two initial surface pressure values. The dotted curves were recorded immediately after displacement and the dashed curves 5 min later; the hysteresis effect is indicated by arrow. The shape of the p-A relation in Fig. 2a is almost identical to that measured at solvent-spread DOPC monolayers [19]. The

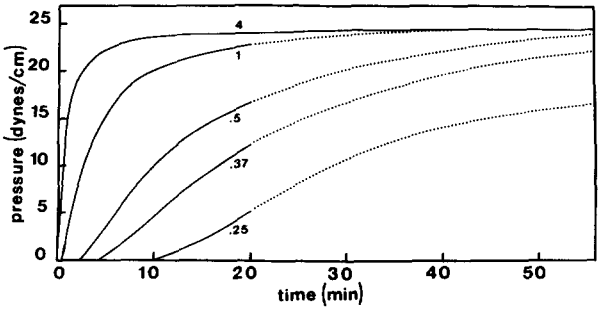

Fig. 1. Surface pressure rise at the interface of a vesicle-containing aqueous solution as a function of vesicle concentration (labels in units of mg/ml).

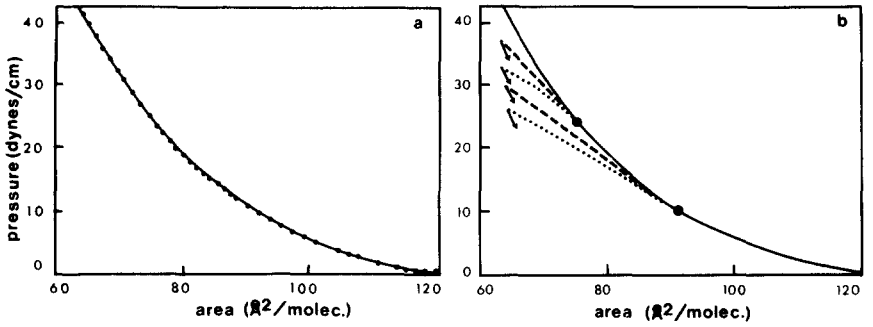

Fig. 2. Relation between surface pressure and area/lipid. Recording was started at time T after shifting the surface layer of the vesicle solution to a compartment not containing vesicles. (a) Recording at T = 60 min. (b) Recordings started at T = 0 (· · · · · ·) and T = 5 min (- - - - - -) for two initial pressure values; the surface area was decreased at the constant rate of 10% initial area/min. The arrows indicate the beginning of a hysteresis loop if the direction of the area change is reversed.

scaling factor which was used in Fig. 2a to translate the surface area into area/lipid was determined from this comparison. However, the area/lipid has been independently estimated using ^{3}H-labelled DOPC. The lipid material at the interface was withdrawn 90 min after displacement of the surface layer. Four independent experiments revealed a lipid content at the surface which corresponded approximately (15% maximum deviation) to that of a DOPC monolayer.

After displacement of the surface layer it first behaves like a lipid monolayer in exchange with a reservoir but slowly transforms into a true DOPC monolayer. The reservoir apparently consists of water-soluble lipid structures rather than of surface-adsorbed lipids in excess of a lipid monolayer. The obvious choice for this reservoir are vesicles or any vesicle-like structures (referred to as surface layer vesicles) which may result from their action as a reservoir. The vesicles either have released a fraction of their lipid content to the surface or some vesicles have disintegrated into surface-adsorbed lipids.

Constant surface pressure

The (equivalent) lipid flux. At constant surface pressure lipid adsorption, desorption or rearrangements within the lipid-vesicle surface organization should generally result in surface area changes necessary to hold the surface pressure at a constant value. These area changes may be formally translated by means of the p-A relation (Fig. 2a) into an equivalent lipid flux ϕ (lipid/cm^2 vesicle chamber surface and per s). This flux shall be used throughout as one way to quantitate the experimental results; whether it corresponds to a true lipid flux to and from the interface or to structural reorganizations within the surface layer does not interfere with its formal definition but is certainly one main question to be answered. The lipid flux is defined positive for area increase (adsorption) and negative for area decrease (desorption).

Time course of the lipid flux. In looking for a defined initial condition (surface pressure) for the flux experiments it was found that the overall system (surface layer plus solution) assumes a vesicle concentration-independent equilibrium state at the surface pressure p_e of 24.5 ± 1 dynes/cm. Besides the

fact that at constant surface area conditions this value was asymptotically approached (Fig. 1), at least at high vesicle concentrations there is other evidence at constant surface pressure conditions: only at p_e zero lipid flux is approached and only at this pressure level a small pressure increase results in desorption flux and a small pressure decrease in adsorption flux. This equilibrium pressure was found to be independent of the vesicle concentration within the range applied of 0.1—10 mg/ml.

The traces in Fig. 3a were recorded after pressure jumps from p_e to lower pressure values (upper three curves, adsorption flux) and to higher values (desorption flux). They were reasonably reproducible for independent experiments and did not depend on the sequence of measurements; if significant deviations occurred, they were generally accompanied by brakes or discontinuities in the curves, indicating the onset of convection, film breakage or leakage across the barriers.

The flux time courses all show a fast and a slow component. The former may arise from relaxations within the surface layer, whereas the latter may be attributed to the vesicle exchange between solution and surface layer. Evidence for the existence of a vesicle exchange was given earlier (cf. text to Fig. 2b). The above assignment is further supported by the observation that only the time course of the slow component was found to depend on the vesicle concentration. Besides the pressure steps applied in Fig. 3a there are many other possibilities, such as the reverse jumps from different pressure values to the equilibrium value. In this case only the fast component is observed at any

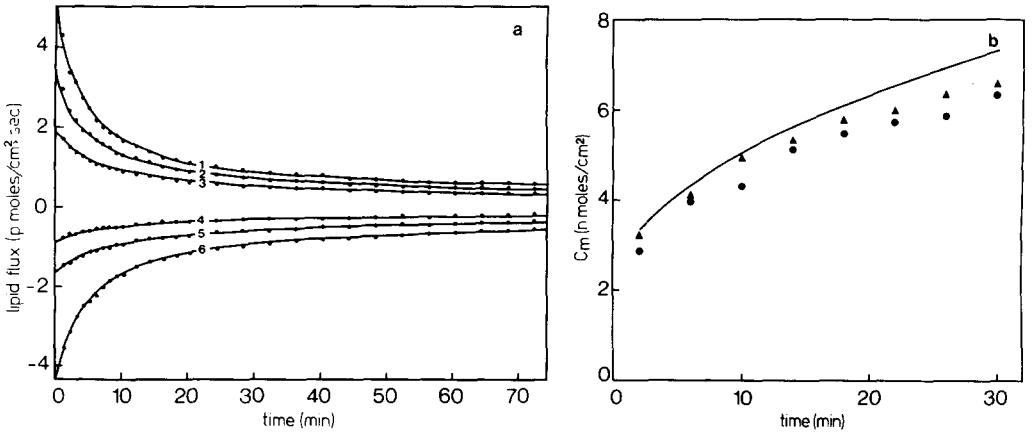

Fig. 3. Time course of the (equivalent) lipid transport to and from the surface at different constant surface pressures. The vesicle concentration was 0.37 mg/ml. (a) Surface pressure ⩾4.8 dynes/cm. Before each recording equilibrium had been reached by applying 24.5 dynes/cm for at least 10 min. The lipid flux (number of lipids transferred to or from the monolayer in 1 s and per cm^2 vesicle chamber surface) is positive if surface adsorption occurs. The numbers 1—6 refer to the surface pressures 4.8, 9.6, 14.4 and 28.8, 33.6, 38.4 dynes/cm. The continuous curves have been calculated. (b) Zero surface pressure. The amount of lipid adsorbed/s per cm^2 vesicle chamber surface at zero surface pressure was measured for two different initial conditions. In one experiment (▲) the surface had been at equilibrium, in the second (●) the surface had been for 30 min at 5 dynes/cm. The scattering of the experimental points is due to the difficulty to determine small amounts of surface lipids at zero surface pressure (for details see Materials and Methods). ———, the theoretical upper limit of adsorption, expected for total disintegration of the surface layer vesicles into lipids at the interface and of any vesicle, which may diffuse to the surface.

initial condition. This lack of any diffusion-like slow relaxation after a pressure jump to the equilibrium pressure indicates that the overall equilibrium can be established just by reorganizations within the surface layer. One may conclude that the number of surface layer vesicles is not affected during surface reorganizations but only their lipid content. The slow relaxation observed at surface pressures unequal to p_e would then be due to the diffusion replacement of the surface layer vesicles by vesicles of normal lipid content. This important conclusion certainly needs further affirmation which will be drawn independently from two other experimental results and from the theoretical analysis.

Hysteresis effect. The lipid flux traces in Fig. 3a indicate a non-linear dependence of the fast decay or rise phase on the surface pressure. From this one may have expected hysteresis effects of the lipid flux during a surface pressure cycle, which indeed were observed. The pattern in Fig. 4a was obtained by measuring the initial flux at eight different pressure values, cycled back and forth between 4.8 and 38.4 dynes/cm in steps of 4.8 dynes/cm, each value held constant for 1 min. The measured flux values follow a hysteresis loop, which slowly shifts to a stable, closed loop, reached after three or four cycles. The closed loop was approached irrespective of the surface pressure at the beginning of the experiment. There was no net gain of surface area during each further cycle (the loop areas for positive and negative flux values are equal). The lipid flux within the surface layer thus is fully reversible. If vesicles would 'vanish' by disintegration into lipids at the interface, the surface area should steadily increase from cycle to cycle because it seems highly improbable that vesicles are 'created', which had to be postulated to account for the observed reversibility.

The slow shift of the hysteresis loop occurred only if the recording was started from a non-equilibrium state within the surface layer; it was absent after pre-equilibration, as shown in Fig. 4c. This hysteresis loop was obtained

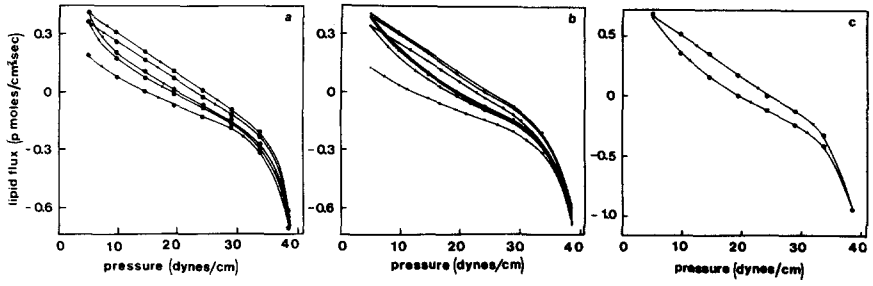

Fig. 4. Hysteresis effect of the lipid flux. The surface pressure was set to eight different values in the cyclic was indicated by arrows. The total time at each pressure (including the transition time between two values of about 3—5 s) was 1 min. The experimental lipid flux values (•) were determined from the surface area changes extrapolated to zero time after each pressure change. (a) Vesicle concentration 0.37 mg/ml. The measurement was started 30 min after filling the vesicle chamber, the surface pressure had reached about 13 dynes/cm (cf. Fig. 1). ———, a handdrawn smooth connection of the experimental points. (b) Theoretical hysteresis loops calculated for the concentration and initial condition of the experiment in (a). (c) Vesicle concentration 0.75 mg/ml. Before the experiment was started the surface layer was at equilibrium. No shift of the hysteresis loop was observed. ———, the theoretical hysteresis for this initial condition.

using a twice higher vesicle concentration than applied in Fig. 4a. The shapes of the two loops are very similar, whereas the flux amplitude increases with increasing vesicle concentration (note different flux scales). The lipid exchange rates thus seem to be concentration independent but the surface concentration of vesicles increases with increasing vesicle concentration.

Zero surface pressure. During the described experiments at constant surface pressure the applied pressures were always equal to or larger than about 5 dynes/cm. At lower (especially at zero) surface pressure, flux measurements revealed qualitative different features of the lipid exchange processes at the surface. This is best illustrated by measurements of the lipid surface adsorption (lipids/cm^2 vesicle chamber) at zero surface pressure. Upon pre-equilibration at surface pressure p_e (Fig. 3b, triangles) the number of surface-adsorbed lipids rose steeply to a high value after the pressure was reduced to a value close to zero. Further adsorption followed a typical (square root) time course of a diffusion-limited surface adsorption. The high-level, reached after about 2 min, is at least one order of magnitude larger than the total lipid content of all vesicles, which could have possibly approached the surface by diffusion. This gives clear evidence that at the beginning of the experiment the vesicle concentration just beneath the surface was much higher than in the bulk solution. A similar result was obtained for another initial condition (Fig. 3b, circles) where the surface pressure had been set to 5 dynes/cm for 30 min before it was set to zero. These two experiments, on one hand, confirm the earlier conclusion that the number of vesicles in the surface layer, once it has formed, stays constant at surface pressures above 5 dynes/cm. On the other hand, they indicate a high vesicle partition towards the surface and the destruction of the surface layer into monolayer lipids if the surface pressure is set to zero.

Other experimental observations further support these conclusions. After measuring a stable hysteresis loop like the one shown in Fig. 4c, the pressure cycle was enlarged to include a pressure well below 5 dynes/cm. The stability of the hysteresis loop was immediately lost, the flux values collapsed to very low values within one cycle and the surface area steadily increased from cycle to cycle. After reducing the pressure cycle again to values above 5 dynes/cm, the original stable hysteresis loop redeveloped in a slow fashion and the surface area changed no more from cycle to cycle.

Theoretical description

The experimental data, in summary, suggest

(a) That the surface layer of a vesicle-containing solution is characterized by a lipid monolayer and a layer of vesicles.

(b) That the vesicles function as a fast lipid reservoir for lipid adsorption and desorption to and from the monolayer, whatever the structural interactions within the surface layer may be.

(c) That the surface layer vesicles are not permanently adsorbed; the resulting vesicle partition is such that the vesicle concentration is higher in the surface layer than in the solution.

(d) That, above 5 dynes/cm, the vesicle partition is not affected (the number of surface layer vesicles stays constant) during lipid exchange with the reservoir,

whereas at zero surface pressure vesicles probably disintegrate during contact with the interface.

The model

From this it is clear that in constructing a model, which may describe the results at surface pressures above 5 dynes/cm, one needs at least four parameters. Two rate constants (k_a, k_d) to describe the lipid exchange between monolayer and vesicle surface layer. One partition coefficient (γ), which describes the excess of vesicles in the surface layer over that in the bulk. At least one fourth parameter is needed to describe the transitions between different states of the vesicle lipid content during its action as a lipid reservoir. The presented data do not allow for any direct conclusion on the number and probability of states a vesicle may adopt during interaction, such as whether the exchange of single lipids or of many simultaneously exchanged lipids is a more appropriate picture. The distribution of vesicle states during lipid exchange with the monolayer may be approached by a population of three states, the minimum number of states which is in formal accord with the conclusions from the experimental data: (1) vesicles equal to those in the bulk solution (c_b); (2) vesicles after release (c_e), and (3) after uptake (c_h) of a quantum of N lipids to or from the monolayer at a certain lipid surface density (c_m). N is the fourth parameter.

If the lipid exchange in the surface layer (between vesicle surface layer and monolayer) is assumed to obey linear first-order differential equations, the reaction scheme reads

$$c_h \underset{k_{d'}}{\overset{k_a}{\rightleftharpoons}} c_b + c_m/N, \text{ and } c_b \underset{k_{d'}}{\overset{k_a}{\rightleftharpoons}} c_e + c_m/N \tag{1}$$

with

$$c_b + c_h + c_e = c_0 \tag{2}$$

The exchange of vesicles between bulk (concentration C) and surface layer may be described by ordinary diffusion. Thus the differential equations to be solved are:

at $x = 0$ (boundary between surface layer and bulk):

$$\partial c_h/\partial t = -c_h k_1 - c_e k_2 + c_0 k_2 + D\partial C_h/\partial x \tag{3}$$

$$\partial c_e/\partial t = -c_h k_3 - c_e k_1 + c_0 k_3 + D\partial C_e/\partial x \tag{4}$$

and at $x > 0$ (bulk)

$$\partial C_h/\partial t = D\partial^2 C_h/\partial x^2 \tag{5}$$

$$\partial C_e/\partial t = D\partial^2 C_e/\partial x^2 \tag{6}$$

with

$$c_{h,e} = C_{h,e} b_0 \gamma, \text{ at } x = 0 \tag{7}$$

and

$$k_2 = k_d = k_{d'} c_m/N; k_3 = k_a; k_1 = k_2 + k_3$$

The variable of interest in comparing theoretical and experimental data is the

lipid flux ϕ between monolayer and vesicles, which can be expressed by the solutions of c_h and c_e:

$$\phi = [\partial c_h/\partial t - D\partial C_h/\partial x - (\partial c_e/\partial t - D\partial C_e/\partial x)] \cdot N \tag{8}$$
$$= [-c_h k_2 + c_e k_3 + c_0(k_2 - k_3)] \cdot N$$

The solutions to Eqns. 2—7 and their derivation are given in Appendix for the initial conditions, which correspond to the experimental conditions investigated.

Evaluation of parameters

It may be briefly outlined how the experimental results are analyzed in terms of the four theoretical parameters. The representation of theoretical curves shown in Fig. 5b allows a direct comparison between theoretical and experimental curves. The composite parameter r is defined as

$$r = \tau_r/\tau_d, \text{ with } \tau_r = k_r^{-1} = (k_a + k_d)^{-1}, \text{ and } \tau_d = \frac{b^2}{4D} = \frac{b_0^2 \cdot \gamma^2}{4D} = \frac{\gamma^2}{C_0^{2/3} \cdot 4D} \tag{9}$$

and describes which process is limiting the lipid flux, either the vesicle diffusion ($r < 1$) or the lipid exchange between monolayer and vesicles ($r > 1$). Most experimental curves could be represented by a theoretical curve with a certain r value to an accuracy shown in Fig. 3a. All r values were smaller than one: the diffusion exchange is slower than the lipid exchange in the surface layer. Experimental results like those in Fig. 3 are first plotted in the representation of Fig. 5b and thus characterized by certain r values. This is illustrated by the dotted curve in Fig. 5b, which corresponds to curve 2 in Fig. 3a; its r value is 0.24. Using either the inset of Fig. 5b or Fig. 5a a value for τ_r is obtained. Eqn. 9 relates r and τ_r to the two unknowns k_r and γ. The two other parameters of the three state model, the exchange quantum N and the equilibrium constant $K = k_a/k_d$ are related to the amplitude of ϕ at zero time by (Eqn. A18):

$$\phi_0 = \tfrac{2}{3} k_r c \cdot N(K-1)/(K+1) \tag{10}$$

This relation does not yet allow a unique determination of N and K_i values from the $\phi_{o,i}$ values in Fig. 3a but it was used to calculate for any N value the corresponding set of K values. The generation of theoretical hysteresis loops finally allows one to determine the most appropriate set of the (N, $K(p)$) values, because its shape is quite sensitive to the choice of $K(p)$.

Results

The theoretical curves in Fig. 3a, which represent the best fit to the experimental points, were calculated using a partition coefficient $\gamma = 75$ and the k_r (p) dependence shown in Fig. 6b. At different vesicle concentrations (0.25, 0.5, 1, 2, 4 mg/ml, at least two experiments each) the k_r profile did not significantly differ from the one in Fig. 6b. The partition coefficient was approximately constant ($\gamma = 75 \pm 10$) between 0.25 and 0.5 mg/ml, whereas it decreased to about 20 at 4 mg/ml vesicle bulk concentration. Using these values for γ and

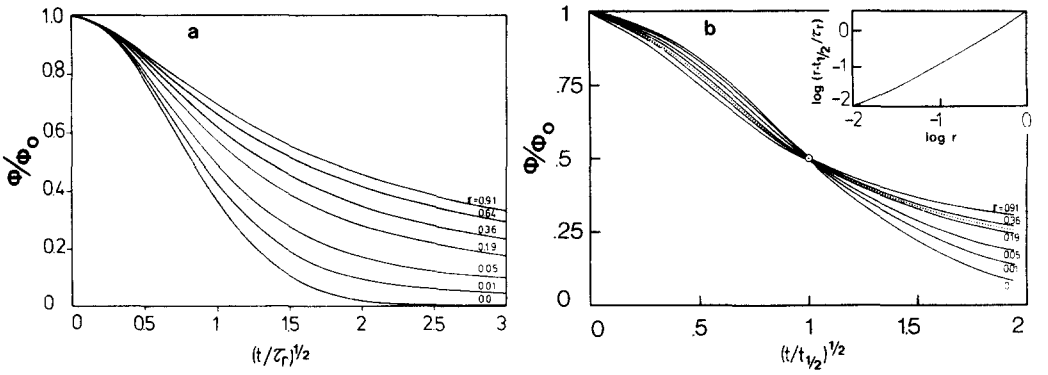

Fig. 5. Calculated time course of the normalized lipid flux for different values of the composite parameter r. (a) These curves are obtained from Eqn. A19. The parameter r describes which process is limiting the adsorption flux ϕ, the vesicle exchange diffusion ($r < 1$) or the surface exchange between vesicles and monolayer ($r > 1$). The curve labelled with $r = 0$ is an exponential decay with the characteristic time τ_r for the lipid exchange. Curves for $r > 1$ are not included simply because they do not apply to the experimental data. (b) The same curves as in (a), but the time scale was redefined (the one in (a) multiplied by $[(t_{1/2}/\tau_r)^{1/2}]$ so that all curves cross each other at half-amplitude. This composite of theoretical curves allows to estimate the r value for an experimental curve, without interference with other parameters. This is illustrated by the dotted curve ($r = 0.24$) which corresponds to curve 2 in Fig. 3a. From this r value and the known half-time $t_{1/2}$ an estimate for the characteristic exchange time τ_r is obtained using the inset of this figure.

k_r (p) theoretical hystereses were calculated for different values of N and $K(p)$. The close agreement between the experimental and the theoretical hysteresis loops, shown in Fig. 4, was achieved with the $K(p)$ dependence in Fig. 6a and the exchange quantum $N = 5 \cdot 10^3$ lipids. The latter value corresponds to 12% of the total lipid content of each vesicle. It is noteworthy from Fig. 4a and b that not only the stable hysteresis loop but also its time evolution is reasonably described theoretically.

Zero surface pressure

It was suggested earlier that at surface pressures close to zero the vesicles

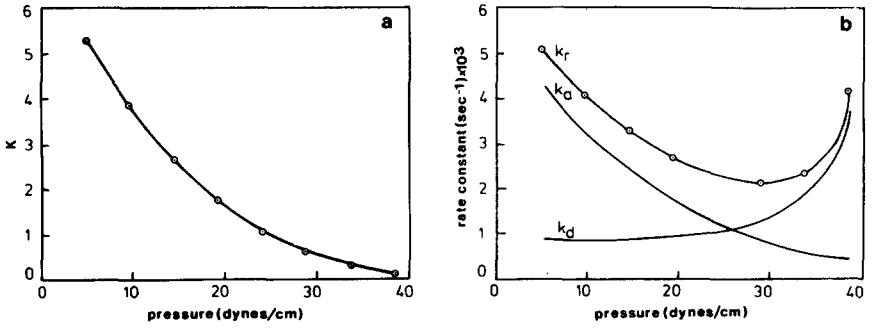

Fig. 6. Pressure dependence of the equilibrium and rate constants which characterize the lipid exchange in the surface layer. The values indicated by circles were obtained from comparisons between experimental and theoretical curves. (a) Equilibrium constant K. (b) Characteristic rate constant k_r, adsorption and desorption rate constants k_a and k_d. The latter two constants were calculated from the relations $K = k_a/k_d$ and $k_r = k_a + k_d$.

probably disintegrate during their interaction with the interface. This hypothesis may be tested by comparing the experimental results in Fig. 3b with theoretical expressions based on total vesicle disintegration. The solid curve in Fig. 3b (calculated from Eqn. A24 in Appendix) describes the case of maximum adsorption: the surface layer vesicles and any vesicle, which approaches the surface by diffusion is assumed to disintegrate totally into surface lipids in times short compared to the diffusion time ($r = \tau_r/\tau_d < 1$). Except for an initial time period of less than 2 min (during this time the adsorption depends on r and τ_r) the time course of this maximum lipid adsorption is fully determined by the given values of the partition coefficient γ and the diffusion coefficient D. The experimental points approach this maximum adsorption curve close enough for one to be quite certain that the vesicles indeed totally disintegrate at zero surface pressure and that there had been a vesicle partition ($\gamma \approx 70$). The remaining deviation is equally well accounted for by small adjustments of γ, D or C and thus is not interpretable.

Constant surface area

Although the derived theoretical relations only apply to constant surface pressure conditions, certain features of the experiments at constant surface area (Fig. 1) may be used to put the proposed model to a further test. On the basis of the earlier summarized conclusions from the experiments the time courses in Fig. 1 are interpreted in the following way. At first vesicles disintegrate. After a certain time (T_1) further disintegration is prevented by the formation of a lipid monolayer with the lipid density $c_{m,o}$. During the sigmoidic pressure rise, the vesicles no longer disintegrate and the vesicle surface layer is built. The surface layer is, at any time, in a fast or pre-equilibrium with the monolayer (τ_r was found to be much smaller than τ_d). When the surface layer is built, approximately after the time τ_d, the further slow rise of pressure, third phase, is explained by the slow equilibration of the vesicle states in the surface layer and in the bulk solution. Finally, at the overall equilibrium, the vesicles before entering and after leaving the surface layer are identical.

The surface pressure measured at time $T_1 + \tau_d$ (T_1 is taken from Fig. 1 at 1 dyne/cm) has been plotted in Fig. 7 as a function of the vesicle concentration.

The theoretical expressions which may correspond to these data at pre-equilibrium are easily obtained from Eqns. 2—7 by setting all diffusion terms to zero. The pre-equilibrium between vesicle surface layer and monolayer is then described by:

$$c_m = c_{m,0} + N_{av} \cdot c_0 \tag{11}$$

with

$$N_{av} = N\left(\frac{1 - K^2}{1 + K + K^2}\right) \text{ and } K = \frac{k_a}{k_d} = \frac{k_a N}{k'_d c_m}$$

C_m and K are related to the surface pressure by Figs. 2a and 6a and $c_{m,o}$ is taken from Fig. 2a at 1 dyne/cm. The resulting prediction of the pre-equilibrium surface pressure as a function of the vesicle concentration (solid upper line

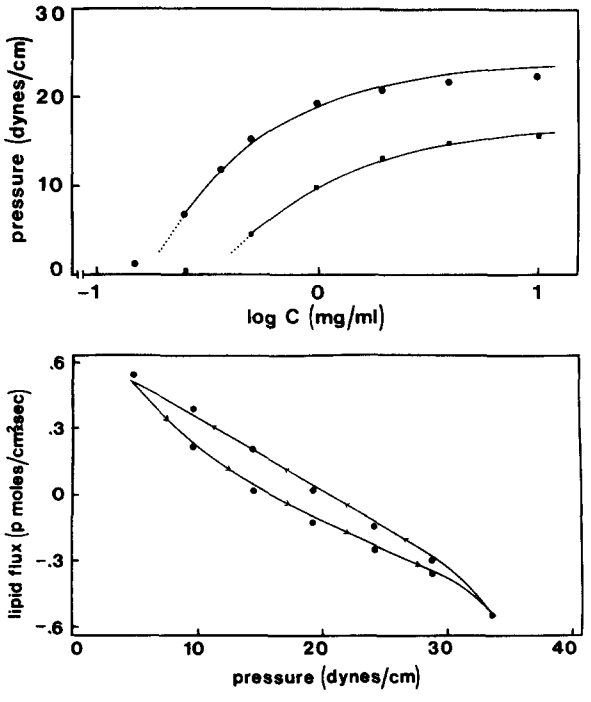

Fig. 7. (a) Vesicle concentration dependence of the pre-equilibrium surface pressure for two vesicle sizes. Upper curve. The experimental data (•) are taken from Fig. 1 at times τ_d (C) (cf. Eqn. 9), at which the surface layer is expected to be just completed by vesicle diffusion from the bulk solution. The surface layer is in a fast (or pre-) equilibrium, the overall equilibrium is not yet reached. The vesicle radius was 35 nm. ———, the theoretical prediction from Eqn. 11, where all variables had been determined using independent experimental data. Lower curve. The same experiments carried out with vesicles of 23 nm radius. ———, calculated from the same parameters used for the upper curve. (b) Lipid flux hysteresis for a smaller vesicle size. This hysteresis loop was measured with vesicles of 23 nm radius at a vesicle concentration of 0.5 mg/ml which may be compared with the hysteresis loop in Fig. 4c for larger (35 nm) vesicles. ———, calculated using the same parameters as in Fig. 4.

in Fig. 7a) is in agreement * with the experiment, which gives confidence both in the underlying concept itself and in its mathematical description.

Vesicle size dependence

The above study refers exclusively to DOPC vesicles of 34.7 nm radius. The same experiments and analysis have been carried out with DOPC vesicles of a smaller size, of 24.5 nm radius. Representative experimental results are shown in Fig. 7a (lower curve) and in Fig. 7b. It is apparent that both the concentration-pressure relation and the hysteresis are similar in shape for the two sizes but shifted to lower surface pressure values for smaller vesicles. The equilibrium pressure p_e was found to be 18 ± 1 dynes/cm. The three state theory accounts for this size-dependent surface activity in a surprisingly simple way. If only one

* Because of the inherent inaccuracies in defining a time at which the surface layer has built but no further diffusion exchange may have occurred (there is always time overlap of these processes) and in defining the critical monolayer concentration $c_{m,o}$ below which the vesicles disintegrate and above which they do not vanish, the close agreement in Fig. 7a seems somewhat accidental.

variable, the exchange quantum N, is changed from $5 \cdot 10^3$ to about $2.5 \cdot 10^3$, the experimental data are fairly well represented by the resulting theoretical curves (solid lower curve in Fig. 7a and b). These data were chosen because they offer a most sensitive test for the right choice of the theoretical parameters. It is important to notice that N is decreased by the same factor as that by which the vesicle (outer) surface area is decreased.

Discussion

Preliminary conclusions from the experimental results, summarized earlier, were used to construct a model for the observed lipid exchange phenomena. The additional assumptions necessary to formulate the theory appear to be quite insignificant (cf. last section of Appendix). Application of the theoretical relations to the experimental results revealed detailed and consistent agreement. This allows for further specifications of the lipid-vesicle surface organization and its rearrangements during lipid transport.

Surface layer structure

The concentration of vesicles, which interact with the monolayer, was found to exceed that (at any plane) in the vesicle solution by a factor of 75. The attractive force, which leads to this high partition, is, at least mainly, of electrodynamic nature (van der Waals force) arising from the sudden change of dielectric properties at the air-water interface. There are many similar, more common examples for the action of this force such as cell-cell or cell-substrate adhesion. Such forces have been calculated for geometries which apply here (for a review cf. Ref. 20). A change of the van der Waals chemical potential of about 4 kT, which corresponds to the observed partition coefficient, can readily be accounted for if the vesicles approach the surface closer than about 1 nm. A close, probably physical contact seems indispensible for the occurrence of lipid exchange: if lipids had to pass through bulk water the exchange rates would be expected to be orders of magnitudes smaller [21] than the figures obtained. The range of this attractive force is small compared to the vesicle size, so that the partitioning may occur between solution and only one layer of vesicles close to the surface. This correlates well with the saturation of the partition coefficient above 0.5 mg/ml vesicle concentration. At this concentration, the number of vesicles in the surface layer corresponds to about one dense layer of vesicles. The surface layer of vesicles may thus be visualized as basically one single layer of vesicles just beneath the lipid monolayer, which is rather densely packed at high vesicle concentrations, although it is in diffusion exchange with vesicles in solution.

Lipid equilibration

As the first step in the spontaneous surface layer formation at the interface of a fresh vesicle solution the vesicles, due to the absence of a monolayer, directly contact the water surface and disintegrate into surface lipids, as it was concluded from experiments at zero surface pressure. The lipid monolayer thus forms until it prevents the vesicles from contacting air upon which the

vesicle partition between surface layer and solution establishes. Now the lipid content within the surface layer is in a fast or pre-equilibrium: the lipid content in the monolayer has increased at the expense of the lipid content of the surface layer vesicles. The latter, however, are slowly replaced via diffusion exchange by 'normal' vesicles from the solution, which again equilibrate with the monolayer. The lipid contents of the monolayer and of the surface layer vesicles thus slowly increase until the overall equilibrium is reached.

There are two possibilities for the apparent change of the lipid content of surface layer vesicles during lipid equilibration: first, both layers of the vesicles function as lipid reservoir, resulting in vesicle size changes. Second, only the outer vesicle layer takes part in the lipid exchange with the monolayer, which implies that internal equilibration (flip-flop) is absent or slow enough so that the vesicle size is preserved. There are two main arguments against the first and strongly in favour of the second possibility. (1) The results obtained for the two vesicle sizes could be accounted for by the same set of parameters, if the exchange quantum N was set proportional to the lipid content in the vesicle. This finding uniquely and only matches with the second concept, that only the outer layer of the vesicle is involved in the lipid transport to and from the monolayer: the state of lipids in the outer layers of two differently sized vesicles is comparable only at similar lipid densities. A transition between the same two density states in both vesicles affords the release or uptake of the same fraction of lipids in both outer layers, which is just the result obtained. (2) Hysteresis loops, measured for the two vesicle sizes should be identical if the vesicle size would change during the cycle. This is expected simply because the vesicles would adjust to the same size cycle; the memory is lost about their original size, which only represents an initial condition. This is in contrast to the experimental results which are quantitatively interpretable by assuming that only the outer layer of the vesicles exchanges lipids with the monolayer.

Overall equilibrium

The experiments at the overall equilibrium revealed an interesting aspect: the independence of the equilibrium surface pressure on the vesicle concentration. Apparently each single vesicle is in equilibrium with the monolayer. Furthermore, the observation that the surface pressure at the equilibrium within the surface layer is different for different vesicle sizes but equal to the overall equilibrium pressure can only be accounted for if the vesicle assumes an internal equilibrium state at its normal size rather than an equilibrium size. Thus, the overall equilibrium is characterized by the internal equilibrium of each surface layer vesicle as such. The monolayer lipid density adjusts to this state. The vesicle size dependence is quantitatively explained by the lipid density concept: any increase or decrease of the lipid density away from the equilibrium density at the vesicle outer layer both result in an increase of the vesicle energy. This increase is larger for the removal of a certain number of lipids from a smaller vesicle than from a larger one due to the increase of the concomitant change of the lipid density. As one consequence, the smaller vesicles are found in equilibrium with a monolayer at a lower lipid density compared to the larger vesicles. It also appears from this that the vesicle size dependence of the equilibrium pressure is not, at least not predominantly, due to the

certainly somewhat different states of the lipids in differently sized vesicles (different curvature) but arises from the finite size of vesicles.

Pre-equilibrium

At pre-equilibrium the surface pressure is dependent not only on the vesicle size but, in contrast to the overall equilibrium, also on the vesicle concentration (cf. Fig. 7a). Both experimental dependences could be accounted for by the theory without any adjustment (the parameters had been determined using data obtained at the overall equilibrium). This is regarded as a detailed justification of the underlying concept, which explains the vesicle size and concentration dependences at pre-equilibrium (Fig. 7) in the following way: the main difference between pre- and overall equilibrium is that the lipid content within the surface layer is limited at the former and saturated at the latter condition. As a consequence the vesicles are not in internal equilibrium at the pre-equilibrium, instead they are in lipid exchange equilibrium with their own loss of lipids to the monolayer. In a series of experiments using increasing vesicle concentrations the loss/surface layer vesicle, needed to develop a certain surface pressure, decreases, so that pre-equilibrium is reached at increasing amounts of surface-adsorbed lipids or at increasing surface pressures. Similarly, with increasing vesicle size a lower surface concentration of vesicles is sufficient to reach a certain fixed surface pressure and the pre-equilibrium surface pressure increases.

Consequences of the lipid density equilibration

There seems little doubt left that only the vesicle outer layer takes part in the lipid flux processes to and from the lipid monolayer. The resulting lipid density changes in the vesicle outer layer offer a unique explanation of the main observations even on a quantitative level. This conclusion puts some restriction to the various possibilities, by which lipids might be exchanged between vesicles and monolayer. If the vesicle would experience a strong structural perturbation in the region of contact with the monolayer, the properties of this area are likely to govern the exchange of lipids and not, as was concluded, the vesicle outer layer as a whole. The same argument applies to the state of the monolayer in the region of contact. It thus seems likely that the main structural characteristics of the vesicle and of the monolayer are preserved even in the region of contact.

How then are lipids exchanged if vesicles and monolayer are not strongly interacting but structurally preserved and even their lipid density not significantly altered in the contact region? One answer to this basically unresolved question is appealing to us. The vesicles are certainly not permanently adsorbed to the monolayer. One therefore has to consider diffusion collisions between the two structures, intensified by the van der Waals attraction of vesicles towards the interphase. The minimum distance between the colliding polar head layers is probably close enough to exclude free water from the contact region. The absence of free water certainly reduces the energy barrier for the lipid hydrocarbon chains to leave one layer and eventually enter the other (the polar head mainly needs to turn). Also, during collisions the lateral pressure due to hydrophobic interactions is transiently at least partly abolished and the hydrocarbon tails gain motional freedom. However, lipid density relaxations

towards lower values within the contact region which might follow this pressure relaxation may be slower than the encounter time, because the lipid exchange was found to be governed by the overall lipid density in the vesicle outer layer.

One may ask at which lipid loss in its outer layer the vesicle becomes unstable. During a typical hysteresis loop (cf. Fig. 4) the deviations from the equilibrium density are less than 5%, whereas longer applications of 5 or 38 dynes/cm (cf. Fig. 3) result in about 12% changes in lipid density. Under these conditions the vesicle appears to be stable; no indication for an induction of lipid flip-flop and thus size changes have been found. Below surface pressures of 5 dynes/cm, probably at about 1 dyne/cm, vesicle disintegration was observed. Here the lipid loss in the vesicle outer layer is estimated to be 15—20%. However, the possibility that disintegration is not caused by this high loss but a direct vesicle-air contact at relatively low lipid monolayer densities cannot be excluded.

The sensitive and quite direct reflection of the lipid state in a vesicle membrane by the well characterizable state of lipids in a monolayer may be used in many connections. So it is very intriguing to use the relation between surface pressure and lipid density at the vesicle surface to evaluate the elastic modulus and to estimate the energy-lipid density relation as well as the intrinsic lateral pressure in the bilayer. These data are of general importance in any description of the bilayer state, they will be discussed in a separate publication.

The described flux experiments and their analysis may develop to a general tool to identify and investigate different basic realizations of interaction and exchange between lipid structures. Its applicability seems not restricted to the use of only one component. Experiments with lipid-protein vesicles (H. Schindler et al., unpublished results) showed that the insertion of proteins from the vesicles into the monolayer may be characterized. The effect of any agent, which is known or suspected to influence either the vesicle or liposome itself (such as by induction of lipid flip-flop) or its interaction with the monolayer (such as by induction of fusion or adhesion), may be studied, as well as the interactions between lipid layers of different compositions.

Appendix

Laplace transformation of Eqns. 3—7 leads to:

at $x = 0$:

$$p\bar{c}_h - c_{h0} = -\bar{c}_h k_1 - \bar{c}_e k_2 + ck_2/p + D\partial\overline{C}_h/\partial x \tag{A1}$$

$$p\bar{c}_e - c_{e0} = -\bar{c}_h k_3 - \bar{c}_e k_1 + ck_3/p + D\partial\overline{C}_e/\partial x \tag{A2}$$

$$\bar{\phi} = N(\bar{c}_h k_2 - \bar{c}_e k_3 - c(k_2 - k_3)/p) \tag{A3}$$

at $x > 0$:

$$p\overline{C}_h - C_{h0} = D\partial^2\overline{C}_h/\partial x^2 \tag{A4}$$

$$p\overline{C}_e - C_{e0} = D\partial^2\overline{C}_e/\partial x^2 \tag{A5}$$

$$\bar{c}_{h,e} = \overline{C}_{h,e} b \text{ at } x = 0 \tag{A6}$$

with $k_2 = k_d = k_d' c_m/N$; $k_3 = k_a$; $k_1 = k_a + k_d$; c = constant.

Eqns. A4 and A5 are satisfied by:

$$\overline{C}_h = A_1 e^{-qx} + C_{h0}/p; \overline{C}_e = A_2 e^{-qx}\, C_{e0}/p \text{ with } p = q^2 D, \text{ and} \tag{A7}$$

$$\bar{c}_h = b \cdot A_1 + c_{h0}/p; \bar{c}_e = bA_2 + c_{e0}/p \tag{A8}$$

Insertion into Eqns. A1 and A2 results in expressions for A_1 and A_2:

$$A_1 = \frac{k_2 c}{b} \cdot \frac{\alpha_1 s - \alpha_2 k_2}{p(s^2 - k_2 k_3)}; \; A_2 = \frac{k_2 c}{b} \cdot \frac{\alpha_2 s - \alpha_1 k_3}{p(s^2 - k_2 k_3)} \tag{A9}$$

with

$$s = q^2 D + q\frac{D}{b} + k_1; \alpha_1 = 1 - \frac{c_{e0}}{c} - \frac{c_{h0}}{c}(1 + K), \text{ and}$$

$$\alpha_2 = K - \frac{c_{e0}}{c}(1 + K) - \frac{c_{h0}}{c}K$$

The term of interest, the flux ϕ is obtained from inverse Laplace transformation of Eqn. A3:

$$\phi = N\left[k_2 b A_1^i - k_3 b A_2^i - c k_2 \left(1 - K - \frac{c_{h0}}{c} + \frac{c_{e0}}{c}K\right)\right] \tag{A10}$$

The inverse transforms $A_{1,2}^i$ are found from $A_{1,2}$ by reducing Eqn. A9 to the sum:

$$A_{1,2} = \sum_{i=1}^{4} \frac{\beta_{i1,2}}{p(q + a_i)} \tag{A11}$$

each term of which is easily transformed. The first step is achieved by writing:

$$A_{1,2} = \frac{k_2 c}{bD}\left[\frac{\alpha_{1,2}}{p(q + a_1^-)(q + a_2^-)} - \frac{\alpha_{1,2}(k_2 k_3)^{1/2} + \alpha_{2,1} k_{2,3}}{p(q + a_1^-)(q + a_2^-)(q + a_1^+)(q + a_2^+)}\right] \tag{A12}$$

which is brought into the form A11 by simple algebraic transformations.

The four values of a are given by

$$a_{1,2}^{\pm} = \frac{1}{2b}\left(1 \mp \left(1 - \frac{1}{r}\left(1 \pm \frac{K^{1/2}}{1 + K}\right)\right)^{1/2}\right) \tag{A13}$$

with

$$K = \frac{k_3}{k_2} = \frac{k_a}{k_d} \text{ and } r = \frac{D}{4b^2 k_1} \tag{A14}$$

Each term in Eqn. A11 has the transform:

$$\frac{1}{p(q + a_i)} \rightarrow \frac{1}{a_i}(1 - w(z_i)) \tag{A15}$$

with

$$z_{1,2}^{\pm} = i(Dt)^{1/2} a_{12}^{\pm} \tag{A16}$$

where $w(z_i)$ is the error function for complex arguments, defined by $w(z) =$

$e^{-z^2}erfc\ (-iz)$ and tabulated in Ref. 22. The flux ϕ can thus be expressed by a sum of complex error functions, for the general initial condition $c_{h,e} = c_{h0,eo}$

The initial conditions were chosen to be the overall equilibrium (except in one experiment, Fig. 3a), which is defined by $K(t = 0) = 1$ or $c_{h0} = c_{e0} = c/3$. In this case the solution to ϕ reads:

$$\phi = \frac{\phi_0}{2}[R^- + I^-v^- + R^+I^+v^+ + G(R^- + I^-v^- - R^+ - I^+v^+)] \tag{A17}$$

with

$$G = \left(1 - \frac{1 - K^3}{2(1 + K + K^2)}\right)\Big/K^{1/2} \text{ and } \phi_0 = NCk_1\frac{2}{3}\left(\frac{K-1}{K+1}\right) \tag{A18}$$

$R^\pm$- and $I^\pm$ are the real and imaginary parts of $w(z_1^\pm)$ and $v^\pm = y/x^\pm$. If the term $K^{1/2}/(1 + K)$ is neglected in Eqn. A13 (this is a good approximation far away from the equilibrium, that is for $K << 1$ or $K >> 1$) Eqn. A17 simplifies to:

$$\phi = \phi_0(R + Iv) \tag{A19}$$

This relation has been used to calculate the curves in Fig. 5, which allow a first approximation of k_1 and r from a direct comparison between these and experimental curves.

Hystereses of ϕ_0 versus p (Figs. 4 and 8) are generated from the recursion relations:

$$\begin{aligned}\phi_{0,n} &= [c_{h,n-1} \cdot k_{2,n} - c_{e,n-1}k_{3,n} - c(k_{2n} - k_{3n})]N \\ &= \frac{k_{1n} \cdot N}{1 + K_n}[c_{h,n-1} - c_{e,n-1} \cdot K_n - c(1 - K_n)]\end{aligned} \tag{A20}$$

with $c_{h}^{e,n-1} = c_{h}^{e,n-2}$ (T_{n-2}), where T_{n-2} is the time the pressure p is held constant at p_{n-2}. In a first approximation the estimate for k_1, see above, is used and the K_n values are adjusted to the shape of the experimental hysteresis. These K_n values are used in Eqn. A17, which results in a second approximation of k_1 and r. The k_1 values, in turn, are applied in Eqn. A20 to calculate a new $K(p)$ dependence. A third approximation was found to be unnecessary under any conditions investigated.

Other initial conditions

If $r << 1$, there are experimental initial conditions, such as the one in Fig. 4a, which may be described by a vesicle surface layer, which is in equilibrium with the monolayer but not with the bulk solution. The initial concentrations $c_{h,0}$ and $c_{e,0}$ are then given by

$$c_{h,0} = c/(1 + K_0 + K_0^2) \text{ and } c_{e,0} = c_0K_0^2/(1 + K_0 + K_0^2) \tag{A21}$$

determined from Eqns. A1 and A2 by neglecting the diffusion terms. K_0 and therefore c_{h0}, c_{e0} are related to the initial surface pressure by the curve in Fig. 6a.

Lipid adsorption at zero surface pressure

If it is assumed that the vesicles disintegrate totally during contact with the

air-water interface with the rate k_a (desorption at $p = 0$ is negligible), the set of differential Eqns. A1—A5 degenerates to the form:

at $x = 0$:

$$\partial c/\partial t = -ck_a + D\partial C/\partial x \text{ with } c = C \cdot b \tag{A22}$$

$$\phi = \partial c_m/\partial t = N_{tot} \cdot c \cdot k_a \tag{A23}$$

at $x > 0$:

$$\partial C/\partial t = D\partial^2 C/\partial x^2$$

The solution is obtained in the way as described above. For the initial conditions of the experiment in Fig. 3b ($c_m = 0$) it is found:

$$c_m = NC\frac{2}{\pi^{1/2}}(Dt)^{1/2} + Nc(1 - 4r)(1 - \phi/\phi_0) \tag{A24}$$

with ϕ/ϕ_0 from Eqn. A19. The second term describes the disintegration of the vesicle surface layer after the pressure has been set from p_e to zero, the first terms accounts for the increase of c_m due to vesicle diffusion from the bulk to the surface.

Model dependence of the theoretical expressions

All theoretical relations were derived assuming three vesicle states. The expression (Eqn. 11) for the lipid exchange equilibrium between vesicles and monolayer may be used to demonstrate the effects of introducing more than three states. This relation is easily generalized to any number of states up to the $(2N + 1)$ state system if the uptake or release of N lipids is described by the exchange of single lipids. If $K(p)$ dependences, which best fit the experimental data, are evaluated for these models, it is readily found that the maximum deviation between these $K(p)$ curves is only about 15%. If in addition to the number of states different state dependences of the transition rates are introduced, one may verify that this has a similar effect as introducing different number of states, that is, the resulting effective $K(p)$ dependence and the effective exchange quantum N are quite insensitive to the particular choice of the state dependence of the rate constants.

Vesicle-vesicle exchange has been omitted in the differential equations. First, this exchange is certainly much less effective than the exchange between vesicles and monolayer where strong van der Waals attractions occur (cf. Discussion). Second, even if it is effective it would result in a diffusion-collision exchange of the vesicle lipid contents in addition to the introduced diffusion replacement of vesicles. This would enhance the velocity of exchange, a somewhat larger diffusion constant would have to be used, but the type of solution of the differential equations would not be changed.

Acknowledgement

This investigation was supported by Grant 3.059-0.76 of the Swiss National Science Foundation.

References

1 Racker, E. (1977) J. Supramol. Struc. 6, 215–228
2 Liposomes and Their Uses in Biology and Medicine (1978) Ann. N.Y. Acad. Sci. 308
3 Miller, C. and Racker, E. (1976) J. Membrane Biol. 30, 283–300
4 Schindler, H. and Rosenbusch, J.P. (1978) Proc. Natl. Acad. Sci. U.S. 75, 3751–3755
5 Papahadjopoulus, D., Poste, G., Schaeffer, B.E. and Vail, W.J. (1974) Biochim. Biophys. Acta 352, 10–28
6 Lucy, J.A. (1970) Nature 227, 814–817
7 Lau, A.L.Y. and Chan, S.I. (1975) Proc. Natl. Acad. Sci. U.S. 72, 2170–2174
8 Maeda, T. and Ohnishi, S. (1974) Biochem. Biophys. Res. Commun. 60, 1509–1516
9 Verger, R. and Pattus, F. (1976) Chem. Phys. Lipids 16, 285–291
10 Pattus, F., Desnuelle, P. and Verger, R. (1978) Biochim. Biophys. Acta 507, 62–70
11 Cubero Robles, E. and van den Berg, D. (1969) Biochim. Biophys. Acta 187, 520–526
12 Arvidson, G.A.E. (1965) J. Lipid Res. 6, 574–577
13 Kuksis, A. (1967) Lipid Chromatographic Analysis (Marinetti, B.V., ed.), p. 279, M. Dekker, New York
14 Ames, B.N. and Dubin, D.T. (1960) J. Biol. Chem. 235, 769–775
15 Batzri, S. and Korn, E.D. (1973) Biochim. Biophys. Acta 298, 1015–1019
16 Kremer, J.M.H., Esker, M.W.J. v.d., Pathmamanoharan, C. and Wiersema, P.H. (1977) Biochemistry 16, 3932–3935
17 Zulauf, M. (1977) J. Mol. Biol. 114, 259–266
18 Phillips, M.C., Hauser, H.C. Paltauf, F. (1972) Chem. Phys. Lipids 8, 127–133
19 Demel, A., Van Deenen, L.L.M. and Pethica, B.A. (1967) Biochim. Biophys. Acta 135, 11–19
20 Parsegian, V.A. and Gingell, D. (1972) J. Adhes. 4, 283–306
21 Seimiya, T. and Ohki, S. (1972) Biochim. Biophys. Acta 274, 15–21
22 Abramowitz, M. and Stegun, I.A. (1965) Handbook of Mathematical Functions, Dover Publications, Inc., New York